

Supporting Information

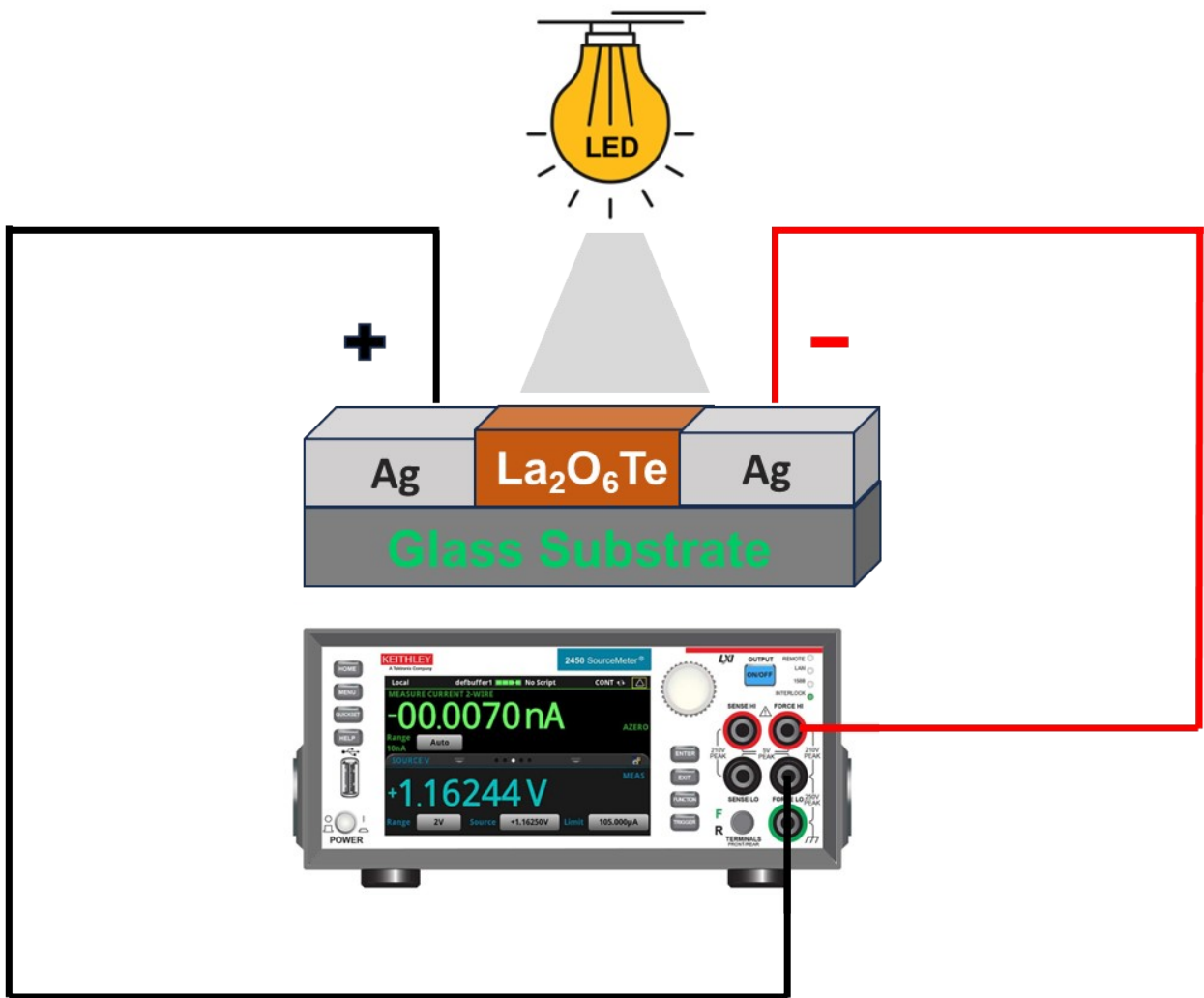
Enhanced Two-Photon Absorption in Hydrothermally Synthesized La₂O₆Te Nanorods for Visible Light Photo Detection

Prabhukrupa Chinmay Kumar¹, Swikruti Supriya¹, Ashutosh Mohapatra¹,
Sripan Chinnaiyah², Ramakanta Naik^{1*}

¹ Department of Engineering and Materials Physics, Institute of Chemical Technology-Indian Oil Odisha Campus, Bhubaneswar, 751013, India

² Crystal Growth and Thin Film Laboratory, Department of Physics, Bharathidasan University, Tiruchirappalli-620024, Tamil Nadu, India

*Corresponding authors: ramakanta.naik@gmail.com



Scheme S1. Detailed photo detection measurement process of the fabricated PDs.

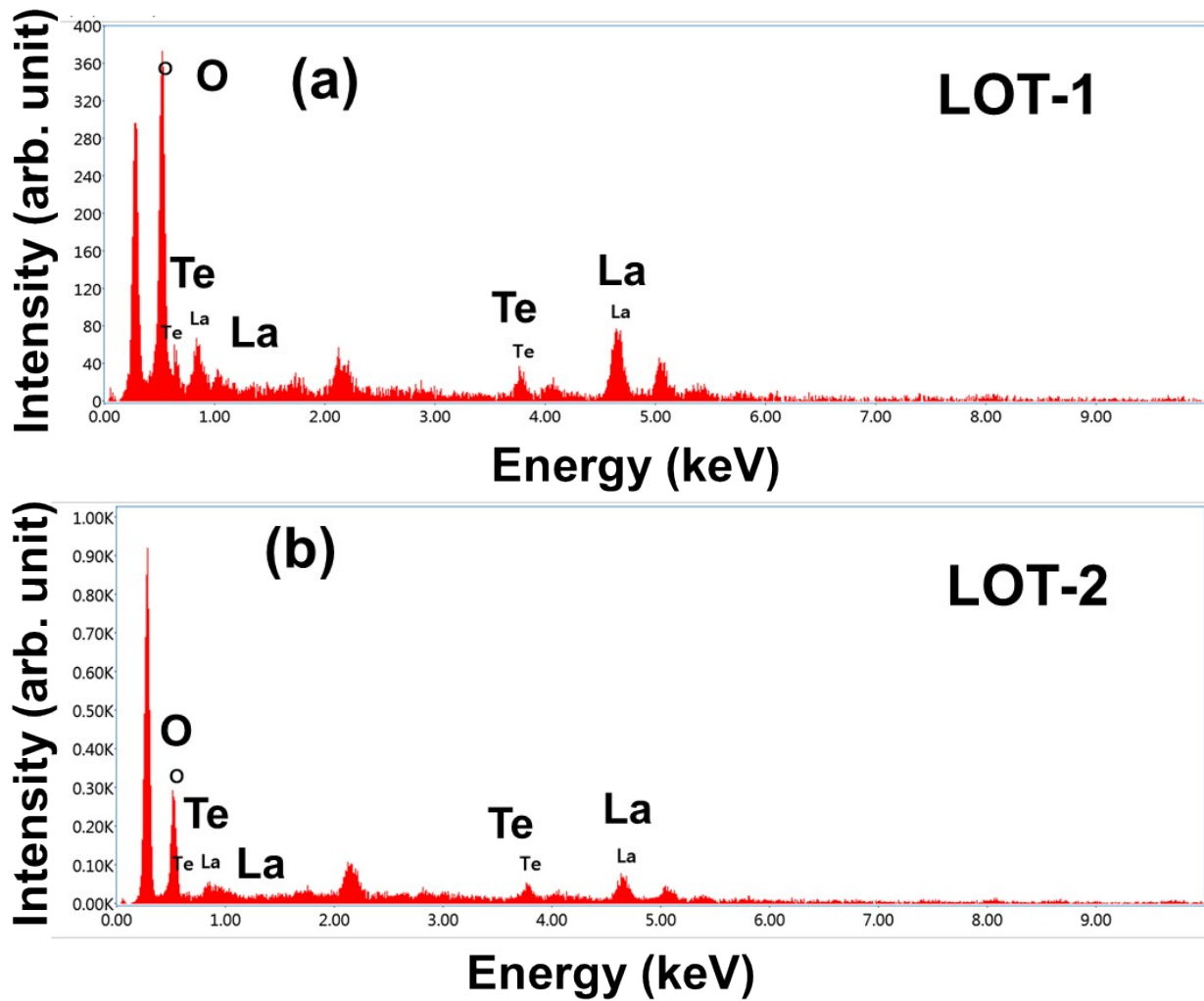


Fig. S1. EDX spectrum demonstrating the components present in each of the produced samples (a) LOT-1, and (b) LOT-2.

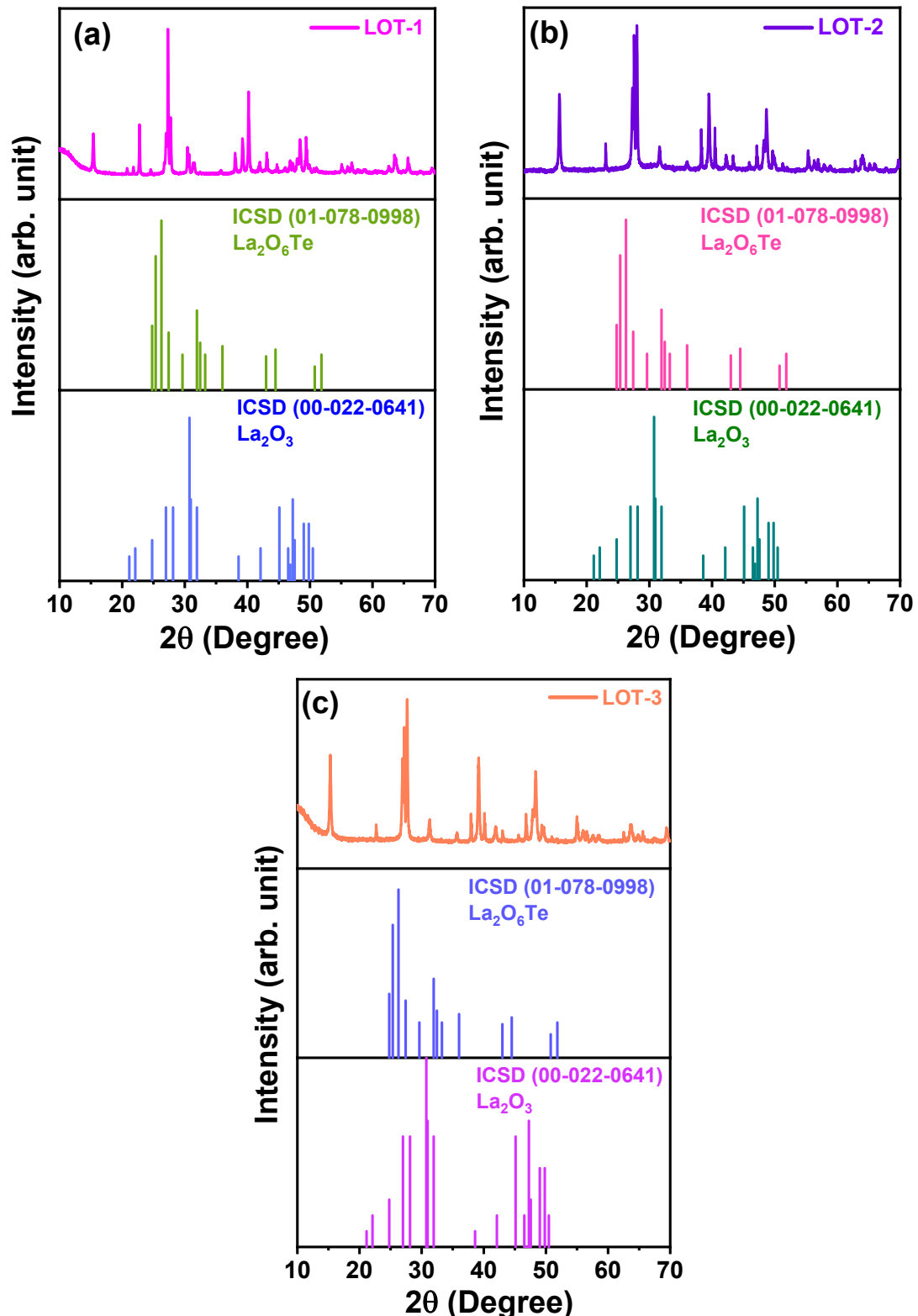


Fig. S2. XRD patterns of individual samples (a) LOT-1, (b) LOT-2 and (c) LOT-3 matched with the respective ICSD cards.

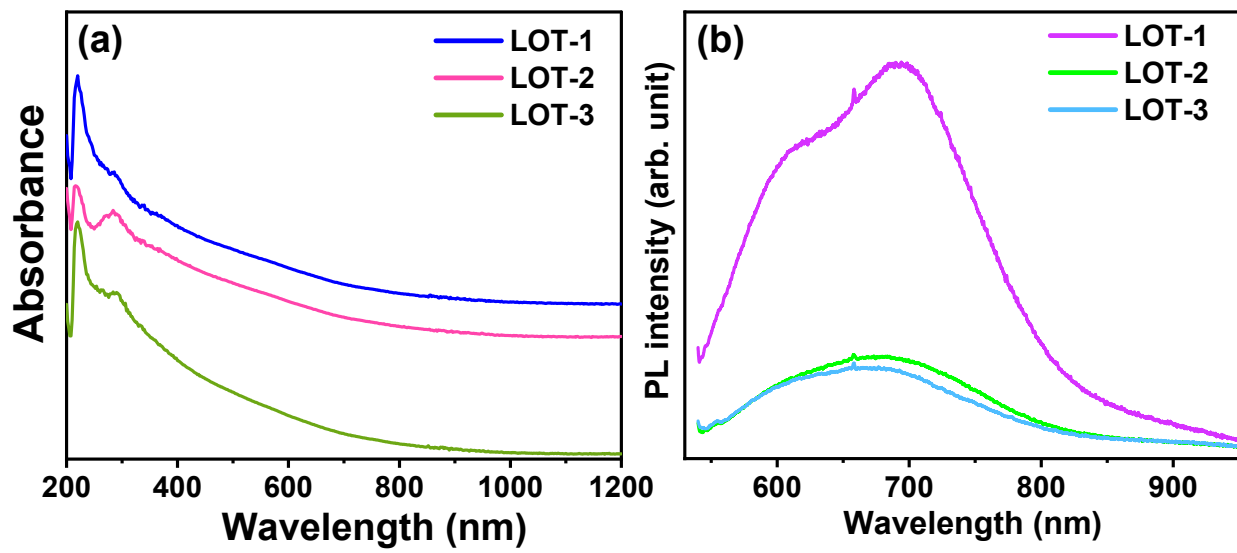


Fig. S3. (a) Absorbance spectra and (b) PL spectra of LOT samples.

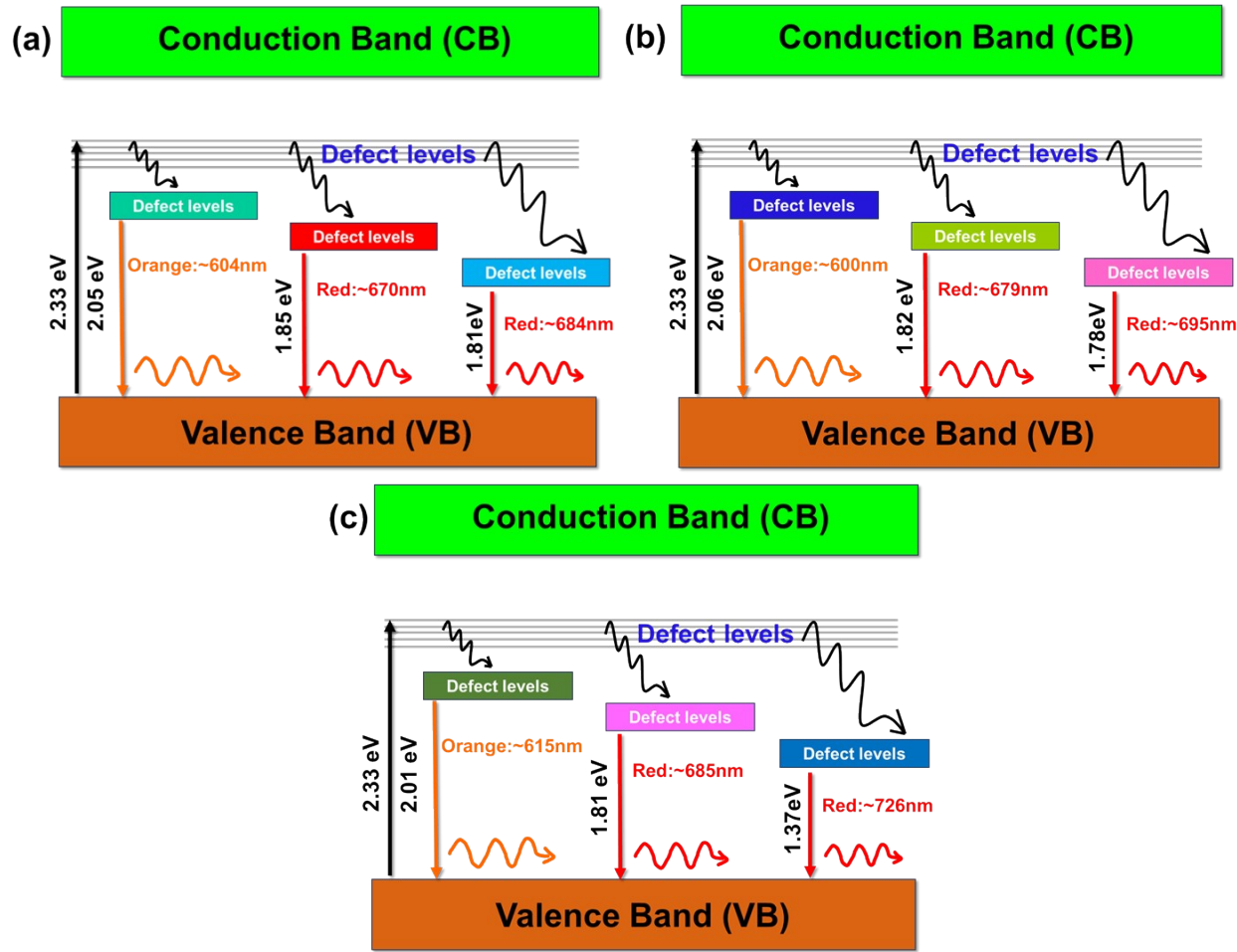


Fig. S4. Schematic illustration of the band gap diagram showing the defect energy states of (a) LOT-1, (b) LOT-2 and (c) LOT-3 samples.

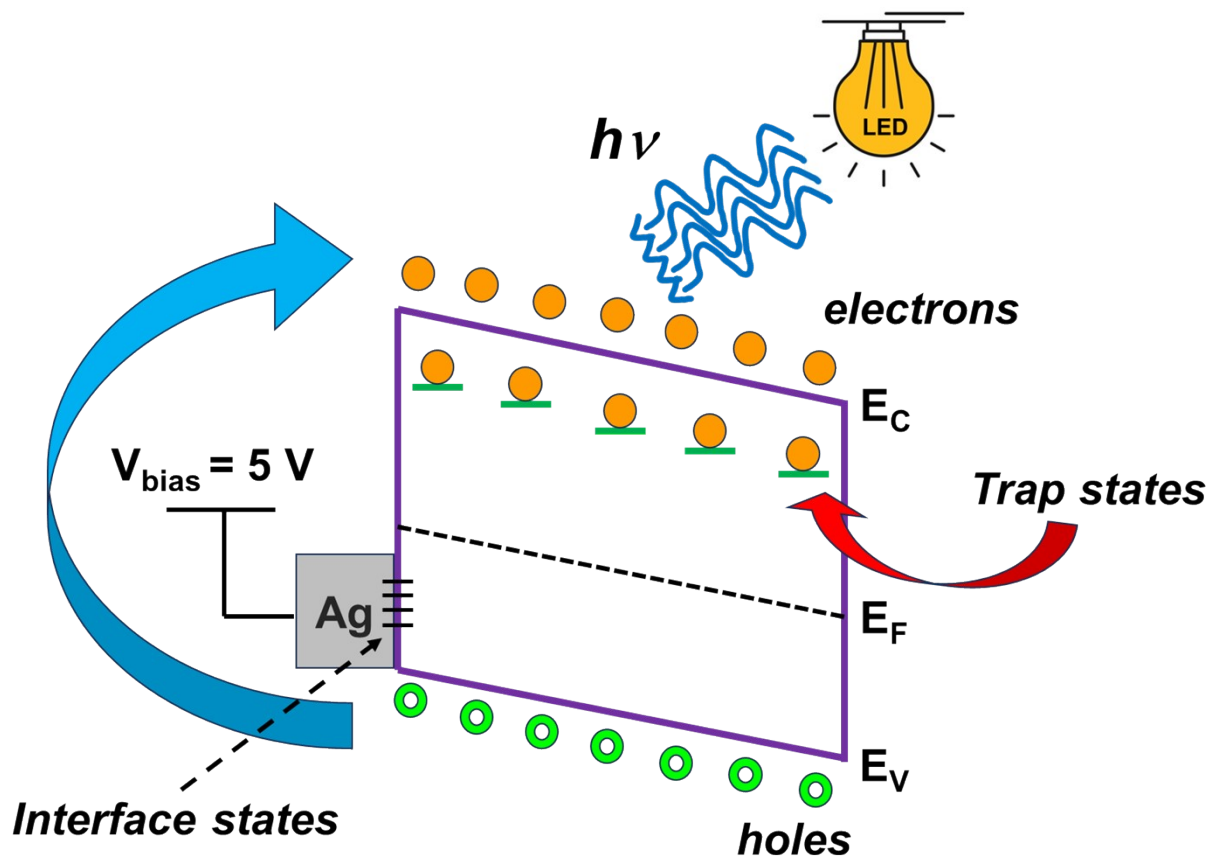


Fig. S5. Schematic diagram of the band structure representing the electron transport mechanism of LOT photodetection process.

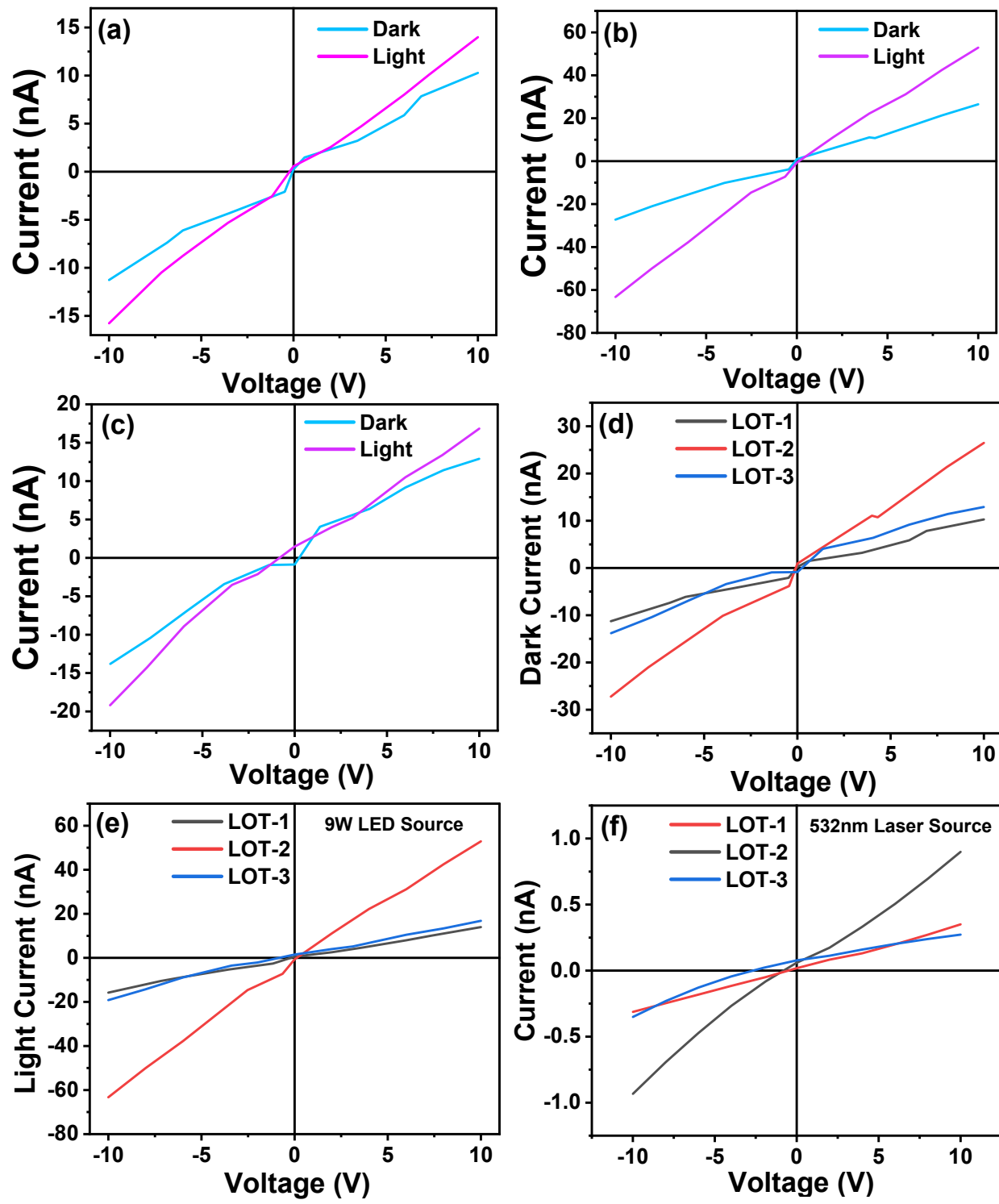


Fig. S6. I ~V characteristic plots showing the combined plot of all the samples in (d) dark circumstances and (e) light conditions, with the linear y-axis of the individual PDs of the sample (a) LOT-1, (b) LOT-2, and (c) LOT-3, respectively.

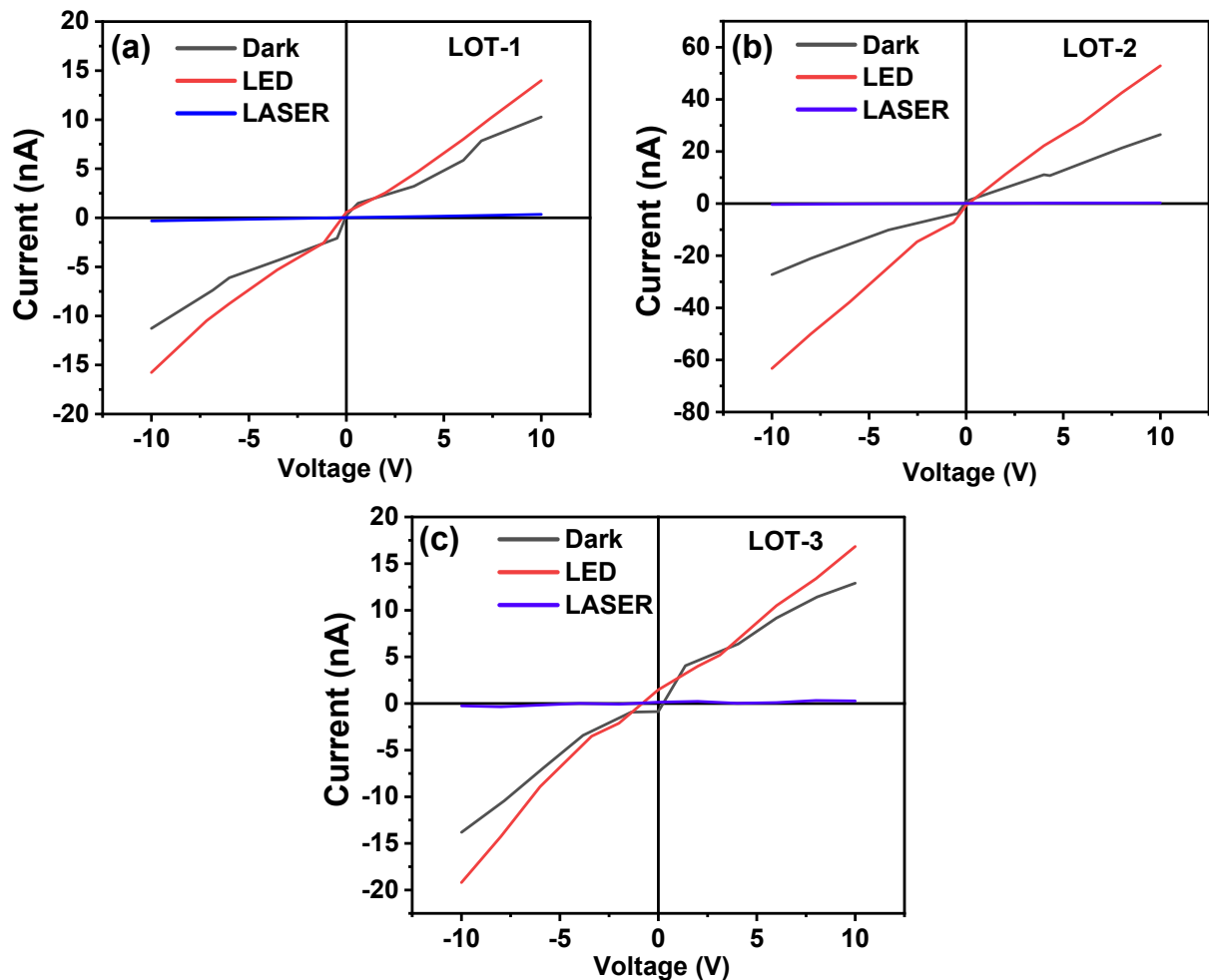


Fig. S7. I~V characteristics plots taken in dark, LED light and 532nm Laser light illumination conditions for (a) LOT-1, (b) LOT-2, and (c) LOT-3 samples.

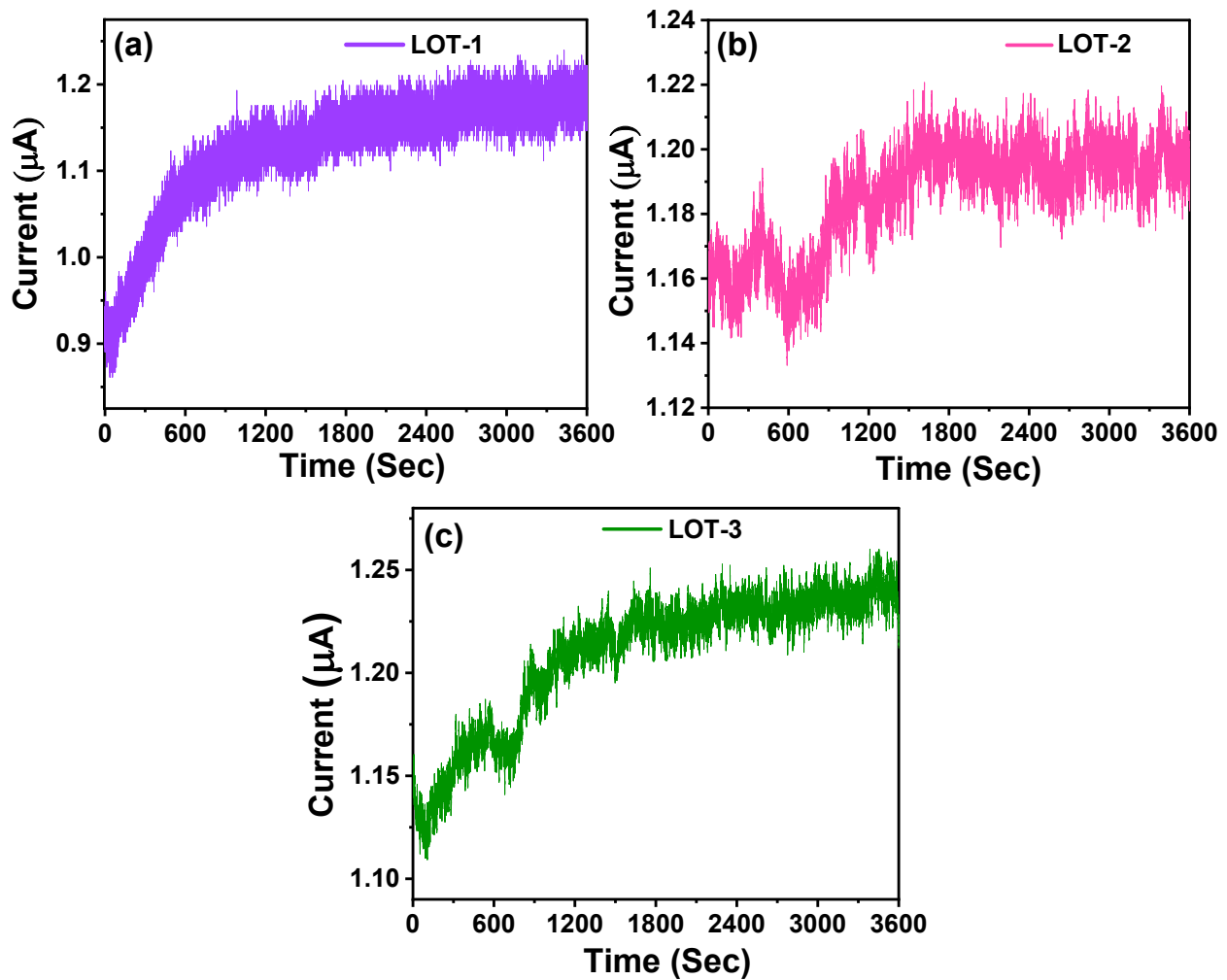


Fig. S8. I~T stability curve of (a) LOT-1, (b) LOT-2, and (c) LOT-3 samples taken for a period of 1 hour.

Table S1. Atomic percentage of various component elements of the samples.

| Sample | LOT-1 | LOT-2 | LOT-3 |
|--------------|--------|--------|--------|
| Element | At. % | At. % | At. % |
| La | 76.82 | 75.32 | 78.73 |
| O | 12.53 | 13.76 | 10.84 |
| Te | 10.65 | 10.92 | 10.43 |
| Total | 100.00 | 100.00 | 100.00 |

Table S2. A summary of the photodetector performances of the typical 2D materials.

| Photodetector materials | Wavelength (nm) | Responsivity (R) (AW ⁻¹) | Detectivity (D*) (Jones) | Refs. |
|-----------------------------------|-----------------|--------------------------------------|--------------------------|-----------|
| Bi ₂ O ₂ S | 850 | 9.48 × 10 ⁻³ | 9.96 × 10 ¹⁰ | 1 |
| Bi ₂ O ₂ Se | 300-900 | 3.712 × 10 ³ | 3.3 × 10 ¹⁰ | 2 |
| Bi ₂ O ₂ Te | 210-2400 | 3 × 10 ⁵ | 4 × 10 ¹⁵ | 3 |
| Bi ₂ O ₅ Te | 400-700 (Vis) | 1.55 × 10 ⁻⁴ | 2.18 × 10 ¹² | 4 |
| GeP | 532 | ~10 ⁻⁴ | 1.38 × 10 ⁷ | 5 |
| O-doped BiI ₃ | 532 | 0.23 × 10 ³ | 2.52 × 10 ¹² | 6 |
| La ₂ O ₆ Te | 400-700 (Vis) | 10.64 × 10 ⁻⁶ | 5.8 × 10 ⁷ | This work |

Table S3. NLO parameters of different materials under performed with CW laser mode.

| Sample Name | β (cm/W) | n_2 (cm ² /W) | $\chi^{(3)}$ (e.s.u.) | References |
|-----------------------------------|------------------------|----------------------------|------------------------|------------|
| N-GO | 0.14×10^{-6} | 5.75×10^{-13} | 3.25×10^{-7} | 7 |
| GO | 2.1×10^{-6} | 1.0203×10^{-11} | — | 8 |
| rGO | 9×10^{-6} | 9.5549×10^{-11} | | |
| CDs | 2.513×10^{-4} | 1.012×10^{-8} | 3.93×10^{-7} | 9 |
| THBSM crystal | 2.014×10^{-3} | 2.324×10^{-7} | 7.504×10^{-5} | 10 |
| CdTe | 1.4×10^{-2} | 2.58×10^{-7} | — | 11 |
| Red-ZnCdSeS | 2.25×10^{-4} | 5.89×10^{-12} | 8.05×10^{-14} | 12 |
| La ₂ O ₆ Te | 3.798×10^{-3} | 3.592×10^{-8} | 5.826×10^{-3} | This work |

Reference

1. P. Rong, S. Gao, M. Zhang, S. Ren, H. Lu, J. Jia, S. Jiao, Y. Zhang and J. Wang, *J. Alloys Compd.*, 2022, **928**, 167128.
2. X. Zou, R. Wang, Y. Sun and C. Wang, *J. Materomics*, 2023, **9**, 10241031.
3. P. Tian, H. Wu, L. Tang, J. Xiang, R. Ji, S. P. Lau, K. S. Teng, W. Guo, Y. Yao and L.-J. Li, *J. Mater. Chem. C*, 2021, **9**, 13713–13721.
4. P.C. Kumar, G.K. Pradhan, S. Senapati, and R. Naik, *ACS Appl. Electron. Mater.*, 2024, **6**, 3311-3324.
5. T. Yu, H. Nie, S. Wang, B. Zhang, S. Zhao, Z. Wang, J. Qiao, B. Han, J. He, and X. Tao, *Adv. Opt. Mater.*, 2019, **8**, 1901490.
6. T. Tian, X. Song, Z. Liu, Z. Ma, B. Wang, B. Wang, X. Li, Y. Yan, Y. Jiang, S. Wei, and C. Xia, *J. Alloy. Compd.*, 2022, **917**, 165429.
7. K. Kumara, T. C. S. Shetty, S. R. Maidur, P. S. Patil and S. M. Dharmaprakash, *Optik*, 2019, **178**, 384-393.
8. K. Kumara, V. S. Kindalkar, F. J. Serrao, T. C. S. Shetty, P.S. Patil and S.M. Dharmaprakash, *Mater. Today Proc.*, 2022, **55**, 186-193.
9. S. Pandiyan, L. Arumugam, S. P. Srirengan, R. Pitchan, P. Sevugan, K. Kannan, G. Pitchan, T. A. Hegde and V. Gandhirajan, *ACS omega*, 2020, **5**, 30363-30372.
10. A. Priyadarshini and S. Kalainathan, *J Mater Sci: Mater Electron*, 2017, **28**, 7401–7412.
11. M. H. Majles Ara, Z. Moslemi, H. Naderi, A. Mihandoost, A. Daneshfar and R. Sahraei, *Applied Physics B*, 2015, **118**, 567-572.
12. Z. Moslemi, E. Soheyli, M. H. M. Ara and R. Sahraei, *J. Phys. Chem. Solids.*, 2018, **120**, 64-70.